Journal of Alloys and Compounds 509 (2011) 5075–5078

Contents lists available at ScienceDirect

Journal of Alloys and Compounds

journal homepage: www.elsevier.com/locate/jallcom

Low temperature pulsed laser deposition of textured γ'-Fe_4N films on Si (1 0 0)

Lei Zhang [a], Tianyu Ma [a], Zubair Ahmad [a], Tianzhi Yuan [a], Cong Lu [b], Yongbing Xu [b], Mi Yan [a,*]

[a] State Key Laboratory of Silicon Materials, Department of Materials Science and Engineering, Zhejiang University, No. 38 Zheda Road, Hangzhou 310027, China
[b] York Laboratory for Spintronics and Nanodevices, Department of Electronics, University of York, YO10 5DD, United Kingdom

ARTICLE INFO

Article history:
Received 19 August 2010
Received in revised form
27 December 2010
Accepted 29 December 2010
Available online 4 January 2011

Keywords:
Iron nitride films
Texture
Low-temperature deposition
Pulsed laser deposition

ABSTRACT

Low-temperature reactive pulsed laser deposition (PLD) was used to prepare iron nitride films. The textured γ'-Fe_4N films with (0 0 1)-orientation were deposited on Si (1 0 0) substrate with Fe buffer layer at a substrate temperature as low as 150 °C. The (0 0 1)-oriented γ'-Fe_4N film grew on the Fe buffer layer with a 3.5-nm thick amorphous interlayer, which eliminated the lattice mismatch stress between them. The films showed a columnar granular morphology with an average lateral grain size of approximately 110 nm. The films exhibited good soft magnetic properties with a high in-plane M_r/M_s value of 0.84. The magneto-optic Kerr effect results indicated an in-plane magnetic isotropy and confirmed the high remnant ratio of the γ'-Fe_4N films.

1. Introduction

Iron nitride compounds have attracted considerable attention, because of their high corrosion resistance, good wear resistance [1] and excellent magnetic properties [2], which make them suitable for applications in magnetic devices. To obtain additional functional properties and to improve the corrosion resistance, magnetic properties and thermal stability, several studies have been carried out on the substitution of Fe atoms by different elements in Fe–N structure [3–8]. γ'-Fe_4N is one of the typical iron nitrides [9–11], which could be applied in magnetic tunnel junctions (MTJs) [12–15] for its high spin-polarized transport [16,17]. In the crystalline structure of γ'-Fe_4N, <0 0 1> axis is the easy magnetization axis [11]; meantime, (0 0 1) plane also shows a highest stiffness in according to elastic constant calculations [18]. Therefore, (0 0 1)-oriented γ'-Fe_4N films are significant for the applications of magnetic film devices.

Recently, molecular beam epitaxy (MBE) and sputtering have been applied to deposit single phase (0 0 1)-oriented γ'-Fe_4N films on various substrates, including MgO (1 0 0) [14,16,19–22], oxidized Si [15,23], $SrTiO_3$ [24], Cu (1 0 0) [25] and Si (1 0 0) [12,13] substrates. However, in previous deposition methods, either high deposition temperature exceeding 400 °C, or high post-annealing temperature above 320 °C were adopted to fabricate high quality (0 0 1)-oriented γ'-Fe_4N films. The high fabrication temperature is incompatible with the production of magnetic devices, i.e. thin film sensors. Pulsed laser deposition (PLD) is widely considered to be a facile technique to grow high-quality metallic films at relatively low deposition temperature, because of the generation of high energetic species and hyperthermal reaction between the ablated cations and the background gas in the laser-induced ablation plasma, which reduce the deposition temperature [26].

In this work, the (0 0 1) oriented texture γ'-Fe_4N films were successfully prepared on Si (1 0 0) substrates by low-temperature reactive pulsed laser deposition technique, which is very important for the integration of ferromagnetic iron nitride magnetic devices with conventional Si microcircuitry.

2. Experimental

The γ'-Fe_4N films were deposited on Si (1 0 0) substrate by PLD technique using a KrF excimer laser (Coherent, COMPerPro201, λ = 248 nm), operating at a repetition rate of 10 Hz with energy density of 5.0 J/cm^2 and using a high pure (99.95%) iron target (Dia: 2.5 cm). The nitrogen gas (99.9995%) was used as nitrogen source for the fabrication of γ'-Fe_4N films. Substrates were placed parallel to the target at a distance of 6.0 cm. The base pressure of 2.0×10^{-7} Torr was obtained with a turbo-molecular pump backed by a rotary pump. Silicon (1 0 0) substrates (1″ size sector wafer) were chemically cleaned by employing standard procedures followed by dipping into dilute HF acid solution in order to get hydrogen terminated oxide free Si (1 0 0) surface, immediately, before loading into the high vacuum chamber. The γ'-Fe_4N films were deposited on Si (1 0 0) wafers following the design [Si (1 0 0)/Fe (20 nm)/γ'-Fe_4N (200 nm)] at a series of substrate temperatures from 100 °C to 200 °C. Before growth of γ'-Fe_4N film, a Fe-layer was deposited on Si (1 0 0) at 100 °C, 1.0×10^{-5} Torr pressure. This Fe layer provided not only a seed layer for the textural growth of γ'-Fe_4N, but also specially used to tune the magnetic properties of γ'-Fe_4N layer for its further applications as ferromagnetic electrodes in MTJ devices. Then, the substrate temperature was elevated to the setting point and the nitrogen gas pressure was increased to 1.1×10^{-2} Torr (13 sccm flow) for γ'-Fe_4N film growth. The deposition rates of buffer layer and γ'-Fe_4N for the all films deposited at different temperatures were approximately 0.04 nm/s.

* Corresponding author. Tel.: +86 571 8795 2730; fax: +86 571 8795 2366.
E-mail addresses: mse_yanmi@zju.edu.cn, mse_yanmi@dial.zju.edu.cn (M. Yan).

0925-8388/$ – see front matter © 2011 Elsevier B.V. All rights reserved.
doi:10.1016/j.jallcom.2010.12.196

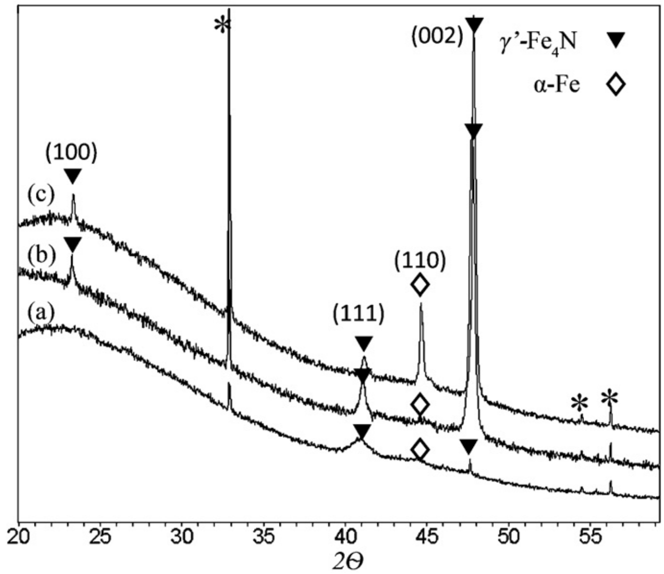

Fig. 1. XRD patterns of the films deposited at various substrate temperatures. (a) 100 °C, (b) 150 °C, and (c) 200 °C. The peaks indexed with asterisks are due to the substrate.

The crystalline structure and crystallographic preferred orientation (texture) were characterized by X-ray diffractometer (XRD, PANalytical X'Pert Pro) using Cu Kα radiation, operating at standard θ–2θ geometry. The film microstructures were examined by Transmission Electron Microscopy (TEM, FEI Tecnai G2 F20) on the cross-sectional section. The surface morphology was observed under an Atomic Force Microscopy (AFM, Veeco Nanoscope 3D). Film thickness calibrations for accurate volume estimation were performed on cross-section images obtained by a Hitachi S-4800 scanning electron microscope (SEM). Magnetic properties were measured by a superconducting quantum interference device (SQUID) magnetometer (Quantum Design MPMS) and magneto-optic Kerr effect (MOKE) with the applied magnetic field parallel to the film plane at room temperature.

3. Results and discussion

Fig. 1 shows the XRD patterns of γ′-Fe_4N films deposited on Si substrate with Fe buffer layer at the temperature ranged from 100 °C to 200 °C. In the case of the films fabricated at 100 °C, the films consist of a mixture of γ′-Fe_4N and α-Fe with poor crystallization quality as confirmed by broad peaks in Fig. 1a, which is due to the limited diffusion mobility of surface atoms at low substrate temperatures. When the deposition temperature was increased to 150 °C (Fig. 1b), all peaks except one weak peak at $2\theta = 44.7°$ were indexed to the γ′-Fe_4N phase. The peak at $2\theta = 44.7°$ might be attributed to the (1 1 0) planes of the Fe buffer layer. The lattice constant calculated from the XRD pattern (Fig. 1b) was 0.3789 ± 0.0002 nm, which is very close to the reported value of γ′-Fe_4N (0.3790 nm) [27]. However, when the substrate temperature was further increased to 200 °C, strong (1 1 0) peak of α-Fe was observed again, besides the peaks indexed to high crystallization quality γ′-Fe_4N phase. It can be concluded that the optimal substrate temperature for the growth of γ′-Fe_4N films is 150 °C under the conditions used here by reactive pulsed laser deposition. Increase or decrease of the substrate temperature will both lead to the formation of α-Fe.

The degree of (0 0 l) preferred orientation of the γ′-Fe_4N film could be evaluated in terms of the Lotgering orientation factor f, which is defined as [28,29].

$$f = \frac{(P - P_0)}{(1 - P_0)} \tag{1}$$

$$P = \frac{I(00l)}{\sum I(hkl)} \tag{2}$$

where P is calculated from the (0 0 l) peak integral intensity to that of the sum of (hkl) integral intensities over a range of 2θ values (20–60°) for γ′-Fe_4N films. Similarly, P_0 was calculated from the standard powder diffraction files of γ′-Fe_4N (Joint Committee on Powder Diffraction Standards (JCPDS) Card No. 06-0627). The calculated Lotgering orientation factor f value for the γ′-Fe_4N phase grew at 150 °C and 200 °C is 0.82 and 0.83, respectively. It indicates that the γ′-Fe_4N film deposited at and above 150 °C had a high (0 0 1)-oriented texture with (0 0 l) planes preferentially oriented parallel to the film plane.

Fig. 2a shows the cross-sectional TEM micrograph of the film deposited at 150 °C, which reveals the columnar microstructure with an average lateral grain size of approximately 110 nm. In the Fe buffer layer, the interlayer spacing is 0.20 nm, which is consistent with that of Fe (1 1 0) planes. In the γ′-Fe_4N layer, the interlayer spacing is 0.19 nm, which is in agreement with that of γ′-Fe_4N (0 0 2) planes as confirmed by corresponding Fourier transformed pattern (the inset of Fig. 2b) from the marked square region in Fig. 2b. The result confirms the (0 0 1)-oriented texture growth

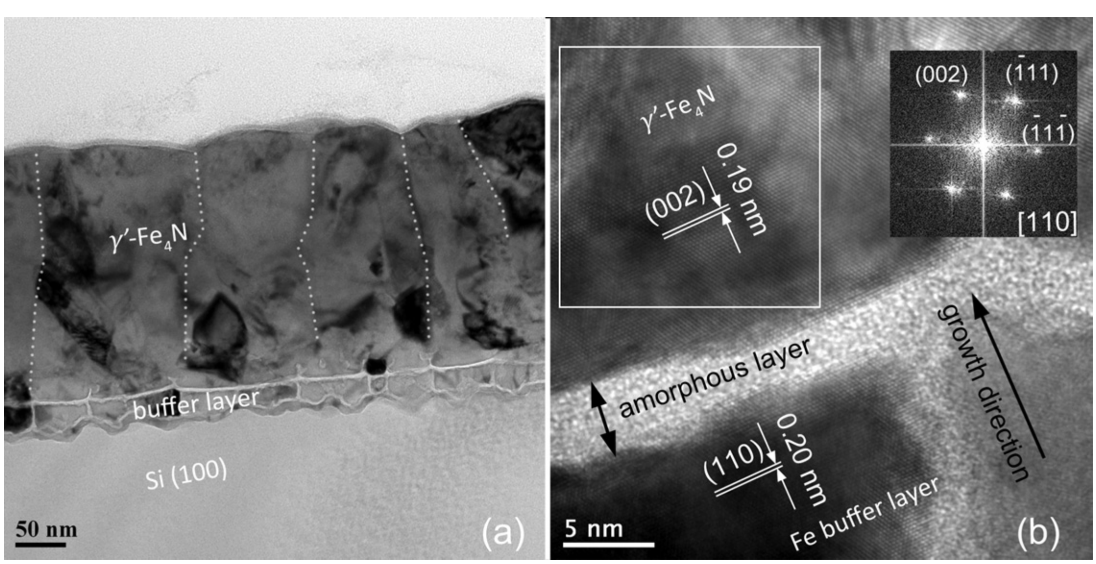

Fig. 2. (a) Cross-sectional TEM micrograph of γ′-Fe_4N film deposited at 150 °C. Weak dotted lines show the boundary of column grains (b) HRTEM image of interface between Fe layer and γ′-Fe_4N layer. The inset in (b) is the corresponding Fourier transformed pattern of γ′-Fe_4N layer.

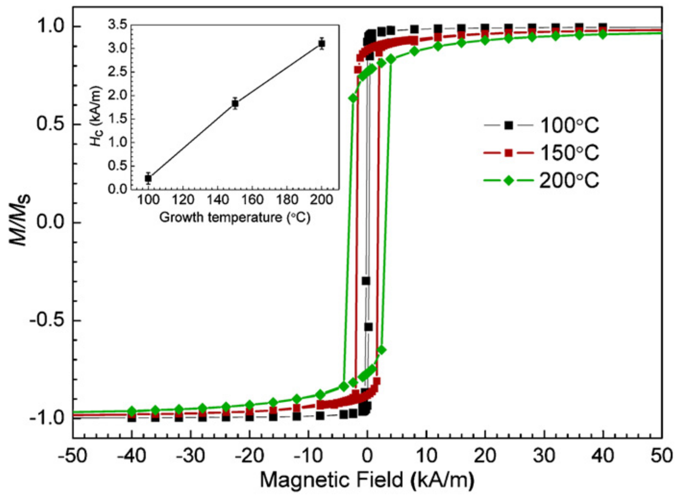

Fig. 3. In-plane magnetic hysteresis loops of the films deposited at various temperatures measured at 300 K. The inset shows the dependence of the coercivity on the deposition temperature.

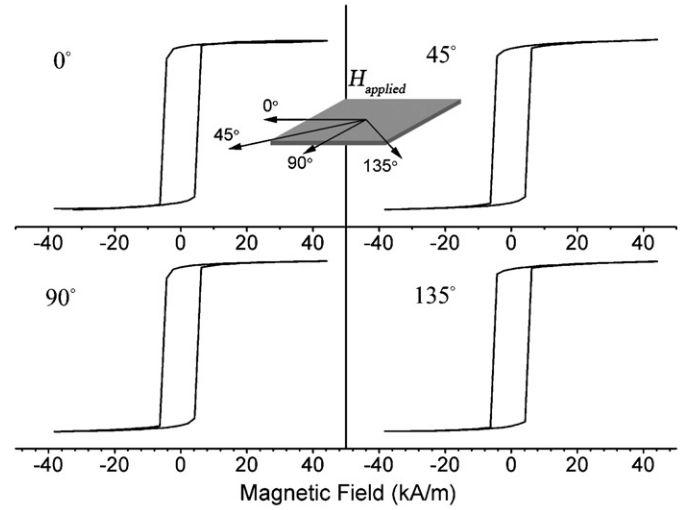

Fig. 4. MOKE hysteresis loops of the γ′-Fe_4N film deposited at 150 °C with the magnetic field applied along four different in-plane magnetic directions. The inset shows the directions of applied magnetic field.

behavior of the as-deposited γ′-Fe_4N films in the present study. It is worthy to mention that there is also an unintentionally amorphous interlayer of 3.5 nm at the interface of Fe/γ′-Fe_4N (Fig. 2b), suggesting no direct epitaxial relationship for the growth of γ′-Fe_4N on Fe layer, which therefore avoids the high interface defects density due to their large lattice mismatch. The formation of amorphous interlayer might be originated from the interface diffusion. In the present work, the big difference in nitrogen composition between the Fe layer and γ′-Fe_4N layer results in the diffusion of nitrogen atoms towards the Fe layer, forming a nitrogen-poor interlayer (nitrogen at.% < 20%) with a gradient distribution of nitrogen composition. In addition, in this nitrogen-poor interlayer region, the nitrogen atoms predominantly occupy the interstitial sites causing the expansion of unit cells, which restricts the long-range ordering in the interlayer. This phenomenon of amorphization of FeN system in nitrogen-poor region has been observed and reported by various researchers [30,31].

Fig. 3 shows the in-plane magnetization hysteresis loops of γ′-Fe_4N films deposited at different substrate temperatures. The inset in Fig. 3 shows the dependence of the coercivity on the deposition temperature. The coercivity seemed to increase with the increase of deposition temperature, which can be attributed to the increase of effective magnetic anisotropy constant. The effective magnetic anisotropy constant value for the film deposited at 100 °C was found to be the lowest due to the presence of the amorphous phase. While, this value for the film deposited at 150 °C was moderately lower than the film deposited at 200 °C, because the magnetic anisotropy value of γ′-Fe_4N (29 kJ/m^3) [20] is less than that of α-Fe (48 kJ/m^3) [2]. The film deposited at 150 °C exhibited good soft magnetic properties possessing a low coercivity (1.83 kA/m) and a large M_r/M_s ratio (0.84). The large M_r/M_s value is speculated due to the (0 0 1)-oriented texture of the γ′-Fe_4N film. The saturation magnetization value (1356 kA/m) of the film deposited at 150 °C is close to the value of pure γ′-Fe_4N (1432 kA/m) reported by Code and Smith [11].

The in-plane magnetic anisotropy properties of the γ′-Fe_4N film deposited at 150 °C were studied by the MOKE hysteresis loops with the magnetic field applied along four different in-plane directions (Fig. 4). As the probing depth of the MOKE technique is around 20 nm, only the γ′-Fe_4N film rather than any underlayer was measured here. The four-direction curves presented almost the same loops, which indicate the in-plane magnetic isotropy of the film. Considering the XRD texture results, it can be concluded that the γ′-Fe_4N film deposited at 150 °C exhibits the fiber texture with c-axis perpendicular to the film surface. The MOKE hysteresis loops are almost square loops, suggesting that magnetization takes place primarily by domain wall motion. The MOKE hysteresis loops also confirm that the γ′-Fe_4N films have a high remnant ratio as observed by the SQUID measurement. The average coercivity observed by MOKE is about 5.17 kA/m, which is significantly larger than the SQUID result (1.83 kA/m). This may be due to the fact that the MOKE is a surface sensitive magnetic measurement technique. In order to study the difference in coercivity, we characterized the film surface morphology by Atomic Force Microscope (AFM). The AFM image included in Fig. 5 shows the film morphology formed by close-packed round grains, and the root mean square (rms) roughness is 10.0 nm measured on a scanned area of 5.0 μm × 5.0 μm, which is approximately 4% of the film thickness. Thus, possible pinning of the domain walls at the surface irregularities is considered to contribute significantly to the larger coercivity in MOKE results.

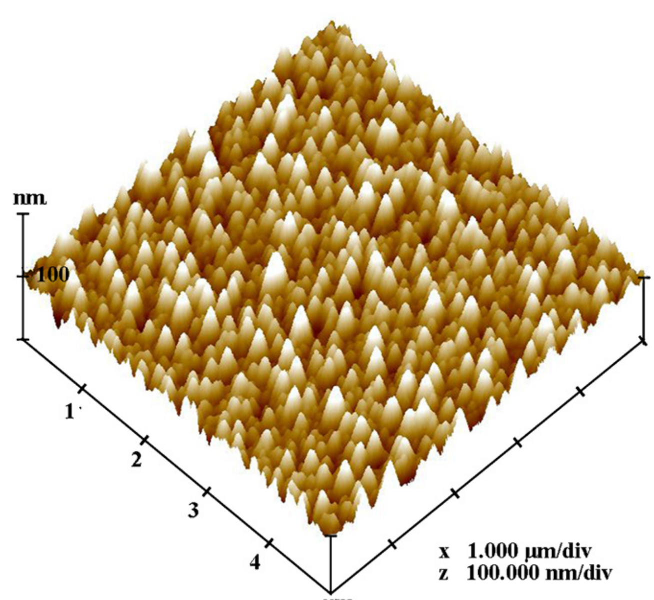

Fig. 5. AFM topography image (5.0 μm × 5.0 μm) of the γ′-Fe_4N film deposited at 150 °C.

4. Conclusions

The (0 0 1)-oriented fiber texture γ′-Fe_4N film was deposited on Si (1 0 0) substrate with Fe buffer layer at 150 °C by low-temperature reactive pulsed laser deposition. Increase or decrease of substrate temperature will both lead to the formation of α-Fe. The (0 0 1)-oriented preferred orientation degree of the γ′-Fe_4N film reaches 0.82. The amorphous interlayer between Fe and γ′-Fe_4N is responsible for the formation of (0 0 1)-oriented texture. In-plane magnetic measurements show the in-plane magnetic isotropy of the film and a large M_r/M_s value of 0.84. The present work describes the deposition of (0 0 1)-oriented γ′-Fe_4N films at a low substrate temperature, which is important for applications in magnetic devices.

Acknowledgment

This work was supported by the National Nature Science Foundation of China (Grant Nos. 50871098 and 50971113).

References

[1] Y. Li, L.A. Wang, D.D. Zhang, L. Shen, J. Alloys Compd. 497 (2010) 285–289.
[2] J. Tang, J. Hong, A. Wu, W. Liu, Y. He, Y. Du, J. Alloys Compd. 479 (2009) 32–34.
[3] L.L. Wang, W.T. Zheng, T. An, N. Ma, J. Gong, J. Alloys Compd. 495 (2010) 265–267.
[4] N. Ma, W.T. Zheng, X. Wang, L.L. Wang, J. Alloys Compd. 477 (2009) 915–919.
[5] S. Atiq, H.S. Ko, S.A. Siddiqi, S.C. Shin, J. Alloys Compd. 479 (2009) 755–758.
[6] X.G. Ma, J.J. Jiang, P. Liang, J. Wang, Q. Ma, Q.K. Zhang, J. Alloys Compd. 480 (2009) 475–480.
[7] S. Kurian, S. Bhattacharyya, J. Desimoni, E. Blanca, A.V.G. Rebaza, N.S. Gajbhiye, J. Phys. Chem. C 114 (2010) 17542.
[8] D. Music, J.M. Schneider, Appl. Phys. Lett. 88 (2006), 031914 (1–3).
[9] L.L. Wang, W.T. Zheng, J. Gong, H.B. Li, X. Wang, N. Ma, P.J. Cao, X.C. Ma, J. Alloys Compd. 467 (2009) 1–5.
[10] R. Niewa, D. Rau, A. Wosylus, K. Meier, M. Wessel, M. Hanfland, R. Dronskowski, U. Schwarz, J. Alloys Compd. 480 (2009) 76–80.
[11] J.M.D. Coey, P.A.I. Smith, J. Magn. Magn. Mater. 200 (1999) 405–424.
[12] S. Isogami, M. Tsunoda, Y. Komasaki, A. Sakuma, M. Takahasi, Appl. Phys. Express. 3 (2010), 103002(1–3).
[13] Y. Komasaki, M. Tsunoda, S. Isogami, M. Takahashi, J. Appl. Phys. 105 (2009), 07C928(1–3).
[14] A. Narahara, K. Ito, T. Suemasu, J. Cryst. Growth 311 (2009) 1616–1619.
[15] K. Sunaga, M. Tsunoda, K. Komagaki, Y. Uehara, M. Takahashi, J. Appl. Phys. 102 (2007), 013917(1–4).
[16] A. Narahara, K. Ito, T. Suemasu, Y.K. Takahashi, A. Ranajikanth, K. Hono, Appl. Phys. Lett. 94 (2009), 202502 (1–3).
[17] S. Kokado, N. Fujima, K. Harigaya, H. Shimizu, A. Sakuma, Phys. Rev. B 73. (2006), 172410 (1–4).
[18] T. Gressmann, M. Wohlschlogel, S. Shang, U. Welzel, A. Leineweber, E.J. Mittemeijer, Z.K. Liu, Acta Mater. 55 (2007) 5833–5843.
[19] T. Takahashi, N. Takahashi, N. Tamura, T. Nakamura, M. Yoshioka, W. Inami, Y. Kawata, J. Mater. Chem. 11 (2001) 3154–3157.
[20] J.L. Costa-Kramer, D.M. Borsa, J.M. Garcia-Martin, M.S. Martin-Gonzalez, D.O. Boerma, F. Briones, Phys. Rev. B 69 (2004), 144402(1–8).
[21] S. Atiq, H.S. Ko, S.A. Siddiqi, S.C. Shin, Appl. Phys. Lett. 92 (2008), 222507(1–3).
[22] R. Loloee, K.R. Nikolaev, W.P. Pratt, Appl. Phys. Lett. 82 (2003) 3281–3283.
[23] M. Tsunoda, Y. Komasaki, S. Kokado, S. Isogami, C.C. Chen, M. Takahashi, Appl. Phys. Express. 2 (2009), 083001(1–3).
[24] K.R. Nikolaev, I.N. Krivorotov, E.D. Dahlberg, V.A. Vas'ko, S. Urazhdin, R. Loloee, W.R. Pratt, Appl. Phys. Lett. 82 (2003) 4534–4536.
[25] Y. Takagi, K. Isami, I. Yamamoto, T. Nakagawa, T. Yokoyama, Phys. Rev. B 81 (2010), 035422(1–8).
[26] R. Eason, Pulsed Laser Deposition Of Thin Films:Applications-Led Growth of Functional Material, Wiley-Interscience, NJ, 2007.
[27] H. Jacobs, D. Rechenbach, U. Zachwieja, J. Alloys Compd. 227 (1995) 10–17.
[28] F.K. Lotgering, J. Inorg. Nucl. Chem. 9 (1959) 113–123.
[29] L.X. Xu, F. Li, Y. Wang, J. Alloys Compd. 501 (2010) 115–119.
[30] R. Gupta, M. Gupta, Phys. Rev. B 72 (2005), 024202(1–12).
[31] S. Chakravarty, M. Gupta, A. Gupta, S. Rajagopalan, A.K. Balamurugan, A.K. Tyagi, U.P. Deshpande, M. Horisberger, T. Gutberlet, Acta Mater. 57 (2009) 1263–1271.